Use of PZT's for adaptive control of Fabry-Perot etalon plate figure

FINAL REPORT to NASA Langley Research Center
For grant **NAG-1-03029**

Wilbert Skinner[1], PI
R. Niciejewski, co-I

Space Physics Research Laboratory
Department of Atmospheric, Oceanic, and Space Sciences
University of Michigan

[1]address:
2455 Hayward St
Ann Arbor, Michigan 48109-2143
Phone: (734)-647-3960
Email: wskinner@umich.edu

June 2005

ABSTRACT

A Fabry Perot etalon, consisting of two spaced and reflective glass flats, provides the mechanism by which high resolution spectroscopy may be performed over narrow spectral regions. Space based applications include direct measurements of Doppler shifts of airglow absorption and emission features and the Doppler broadening of spectral lines. The technique requires a high degree of parallelism between the two flats to be maintained through harsh launch conditions. Monitoring and adjusting the plate figure by illuminating the Fabry Perot interferometer with a suitable monochromatic source may be performed on orbit to actively control of the parallelism of the flats. This report describes the use of such a technique in a laboratory environment applied to a piezo-electric stack attached to the center of a Fabry Perot etalon.

1. INTRODUCTION

High-resolution spectroscopy provides an essential remote sensing diagnostic tool for measuring the composition and thermodynamic properties of atmospheric regions. Long-term synoptic observation schemes in space use non-invasive techniques that take advantage of feeble airglow emissions or absorption signatures. A stable and reliable instrument for recording spectral line shape profiles is the Fabry Perot interferometer. The University of Michigan has successfully flown three Fabry Perot interferometers to observe fundamental geophysical properties of the terrestrial atmosphere: the DEFPI aboard the Dynamics Explorer 2 spacecraft in 1979, the HRDI aboard the Upper Atmosphere Research Satellite in 1991, and the TIDI aboard the Thermosphere Ionosphere Mesosphere Energetics and Dynamics spacecraft in 2001. In all cases, the Fabry Perot etalons were launched successfully, primarily due to extreme care in mounting and maintaining the etalon flats in their respective holders. Once in orbit, the operation of the interferometers proceeded without instrument degradation providing long-term series of measurements of atmospheric dynamics, temperatures, and minor species composition until either satellite re-entry (DE2), termination of mission (UARS), or continuing present day operation (TIMED).

A Fabry Perot etalon consists of two parallel flat semi-transparent mirrors separated by a fixed distance[1]. A monochromatic beam impinging on the etalon flats will suffer multiple beam interference effects after undergoing repeated reflections between the two mirrors. Typical gap separations for airglow emission spectroscopy are on the order of 1 cm. The corresponding free spectral range, or the spectral region free of ambiguity in wavelength, for a HeNe laser (6328 Å) is 0.2 Å, an extremely small fraction of the emitting wavelength. In terms of line of sight velocity, the free spectral range translates to 9500 m/s. Typical airglow measurement specifications require simultaneous temperature and horizontal motion observations with a precision of 10 K and 5 m/s respectively, with a time resolution of 10 minutes given a zenith emission brightness of 100 R. Optimum operational parameters[1] that satisfy these requirements are an etalon reflectivity of 80% and an etalon diameter of at least 10 cm, using a simple photomultiplier tube and aperture as the detecting element. The mirror coating reflectivity corresponds to a reflective

finesse of 14, and for near-ideal behavior, the surface finesse must be at least four times better, or approximately 50. The latter implies that the flatness of the plates must be $\lambda/100$ against curvature defects. These tolerances are fully realizable for ground based Fabry Perot interferometer systems, but space based applications require significant protection against the severe vibrational stress imposed by launch conditions.

An example of the rigors imposed by space qualification requirements is given by the HRDI experiment. The HRDI etalons were chosen for high throughput and high spectral resolution. The etalon reflectivity specification was 90% corresponding to a reflective finesse of 30. The etalon flats were true to a specification of $\lambda/200$. However, measurements obtained once the flats were installed in the special launch mount indicated the overall finesse had been reduced to 12^2. The mount and the mounting process significantly distorted the etalon. Measurements of the effective finesse of the TIDI etalon also indicated a significant sacrifice in performance with a reduction in the overall value from 15 to 8^3.

The opportunity to actively control the parallelism of an etalon in space by adjusting the plate figure presents an exciting opportunity to recover some of the performance loss. The HRDI experiment provided the first space-based control of etalons via piezo-electric stacks attached to the perimeter posts of the medium and low resolution etalons. This report describes a unique test in which an etalon was constructed by placing three Zerodur posts along the perimeter in optical contact against two semi-transparent glass flats, and then placing a piezo-electric stack on the center of the etalon.

2. EXPERIMENTAL SETUP

A schematic diagram of the etalon is shown in Fig. 1. The etalon plate material is Spectrosil-B and the semi-transparent coating uses multiple stacks of ZnS and ThF_4. The design range for 90% reflectivity of the etalon is $6300 < \lambda < 7700$ Å. The plate diameter is 13.2 cm while the coated diameter is 9.4 cm. The Zerodur posts, 5.0 mm in length, are in optical contact with the glass flats at three points along the perimeter separated by 120 degrees. The etalon was placed into a holder that is identical to those flown in the HRDI experiment, thereby imitating the mounting stresses exerted upon the glass plates. Fig. 2 provides a view of the mount with the etalon. Adjustment screws placed above the posts may be seen on the left side of the mount. These are used to press down on the Zerodur posts to adjust the parallelism of the plates.

A bar was securely attached to the left side of the etalon mount of Fig. 2 over the diameter of the etalon. In the center, a piezo-electric stack was attached, with epoxy, with its active faces against the bar and the glass flat. Care was taken to ensure nearly zero force was placed against the etalon itself. The stack, a Thorlabs AE0505D16, is 20 mm in length with a square active area 6.5 mm per side. A Thorlabs MDT694 single-channel piezo-electric controller controls the device. The stack is capable of a maximum displacement of 17.4 μm given a maximum driving voltage of 150 V. The capacitance of the stack is 1.40 μF with a clamping force of 850 N. Operation above 100 V was performed only sporadically to extend the useful life of the stack.

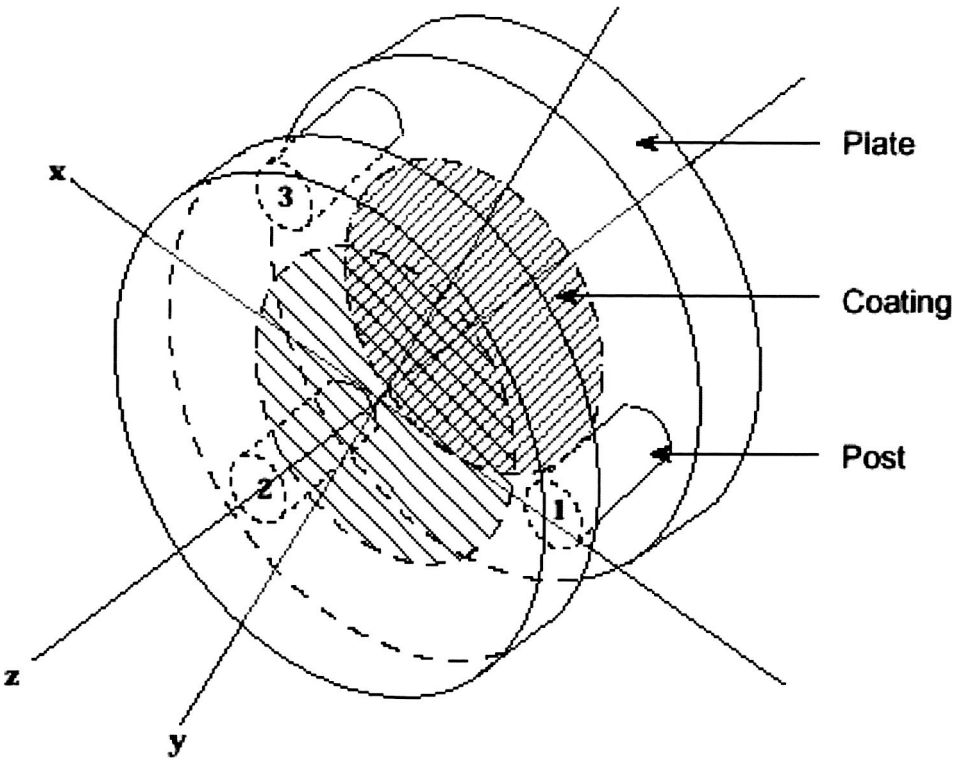

Fig. 1. Schematic diagram of a Fabry Perot etalon. The optical axis is labeled *z*. The posts are in optical contact with the two semi-transparent glass plate flats and are separated by 120 degrees.

The re-configured etalon and mount were secured onto a vertical optical breadboard with the mirrored portions of the glass flats perpendicular in a horizontal orientation. A 12" integrating sphere, with a 4" aperture, was mounted above the etalon. The sphere was illuminated with a Coherent Model 200 single frequency 1.0 mW Class II CW HeNe laser. An aperture wheel was placed between the integrating sphere and the etalon. The setup is shown in Fig. 3. The vertical breadboard was mounted on a horizontal optical bench. Beneath the etalon, a first surface mirror mounted at a 45-degree angle was placed to bend the beam through a 100 mm diameter plano-convex lens with a focal length of 600 mm. A CCD system from Princeton Instruments was placed at the focal plane of the lens. The detector, a CCD02-06 device from EEV with 22 μm square pixels arranged in a 576 x 384 rectangular array, was operated in a slow readout mode, 150 kHz ADC, at 16 bits resolution. A small shutter placed in the optical path determined the integration period. The CCD was housed in a Princeton Instruments TEA/CCD-500-3 mount which had both forced air and liquid cooling. A Neslab RTE-140 cooler circulated water at 5 °C through the CCD housing. The CCD was controlled by a Princeton Instruments Model ST-138S detector/controller, with EPROM version 46. The combined cooling kept the CCD at –50 °C. Though the CCD housing was evacuated to 10^{-4} torr pressure, a small muffin fan placed next to the CCD housing was required to keep condensation from forming on the housing window.

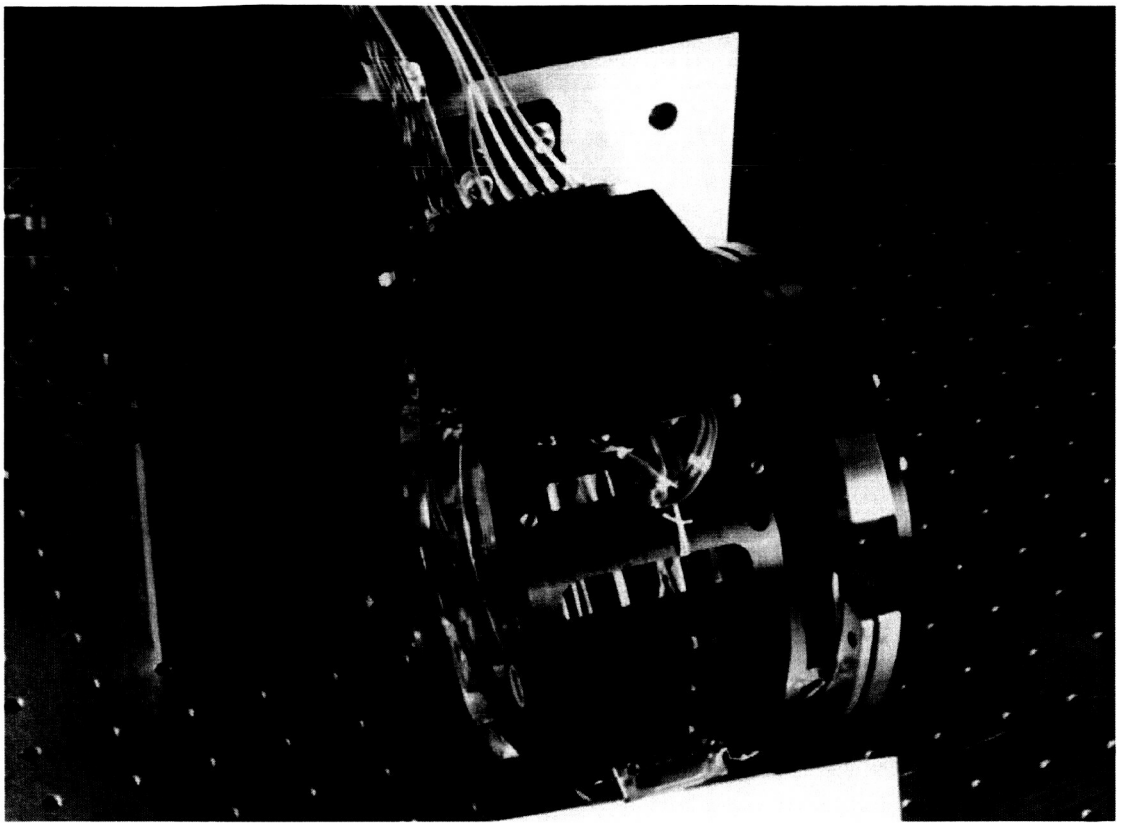

Fig. 2. The mount for the Fabry Perot etalon. The design is identical to that used in the HRDI experiment.

A small PC running either Windows 95 or MS-DOS controlled the experiment. Under Windows 95, the CCD used a vendor supplied display and control program, Win Spec 1.3A. This provided an excellent environment for initial CCD setup and alignment but was unsatisfactory for long-term control of auxiliary peripheral devices. An older program also supplied by the vendor, CSMA v2.2, permitted both control of the CCD and the piezo-electric stack, the latter via an external 0-10 VDC level supplied through a Keithley-Metrabyte DAC-02 interface card. The interface between the CCD controller and the PC was a high-speed ISA card operating at full frame readout.

Software control of the CCD and the piezo-electric stack was achieved through MS-DOS. A macro was created that alternately exposed the CCD for 1 second, read the image with 2x2 on-chip binning, stored the image onto a hard disk file, and then ran an MS/C routine which applied a new D/A DC voltage to the piezo controller. This macro ran for voltages from 0 to 10 VDC at 1 VDC separation and the controller converted this input into 0 to 150 V to the piezo-electric stack. Once a run was completed, the images were processed to 1) determine the center of the fringe pattern, and 2) reduced to spectra using a simple radial reduction routine[4]. Further analysis was performed using MS Excel.

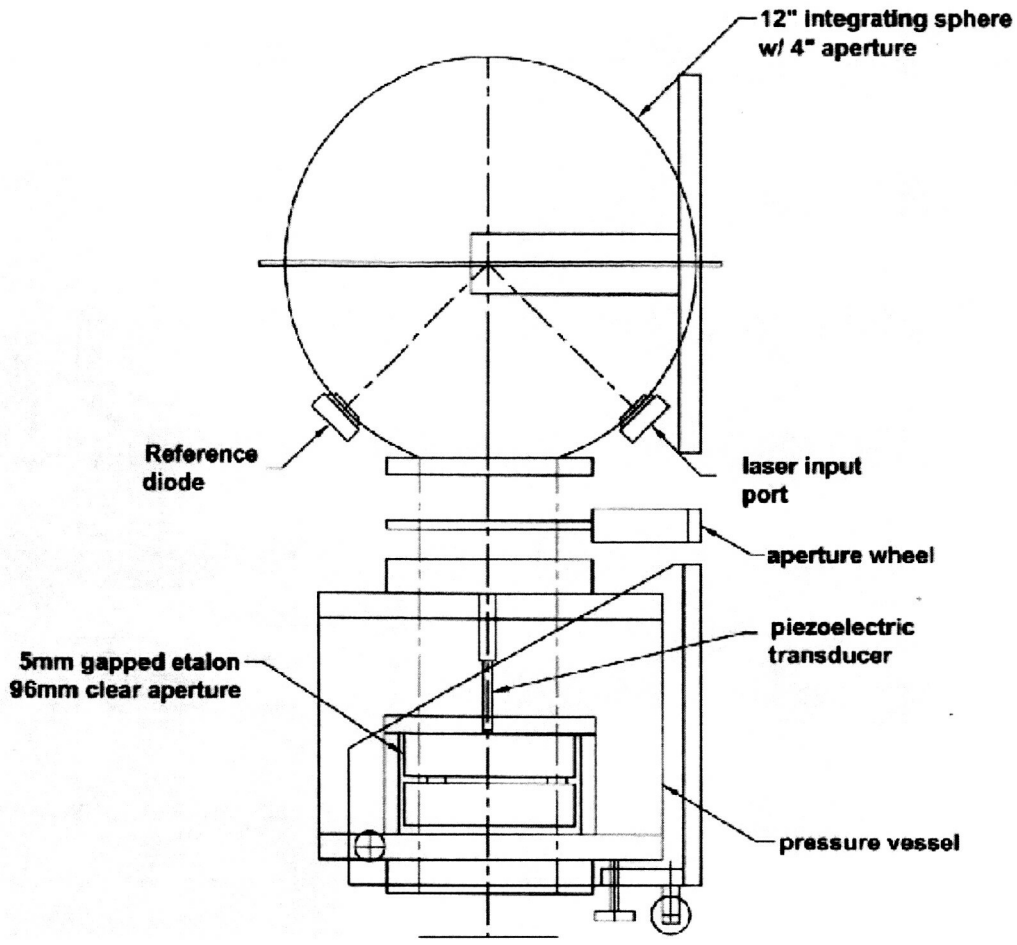

Fig. 3. Experimental setup for viewing diffuse HeNe laser radiation. The etalon is mounted with its glass flats in a horizontal orientation beneath an integrating sphere with a 4" aperture. Both components are securely attached to a vertical optical breadboard.

3. RESULTS

As higher voltages were applied to the piezo-electric stack, the central region of the upper plate contracted forcing the plate gap to narrow. This translated into a reduction in the diameter of the bright fringe patterns. A sample sequence has been converted into an animation and may be viewed by pointing an Internet browser to http://www-personal.umich.edu/~niciejew/full_aperture.gif . Fig. 4 displays the start and end frames of the animation. The full range over which the stack could be controlled was sufficient to scan over a significant fraction of one free spectral range. The analysis of the imagery began by locating the fringe center of the first fringe, the top of Fig. 4. The program accepts an initial guess from the user and then searches away radially from the center in both the x and y axes, in both the positive and the negative directions, to find the pixel with the greatest count rate. This search is performed for 10 rows and columns on either side of the initial guess, and a new center is determined by the average location of positive and negative peaks along the orthogonal axes. This iteration continues until no

further improvement is obtained in the center location. Spectra are formed by collapsing the fringe images onto an r^2 grid, assuming azimuthal symmetry, with radial bin number enumerated from the just determined center.

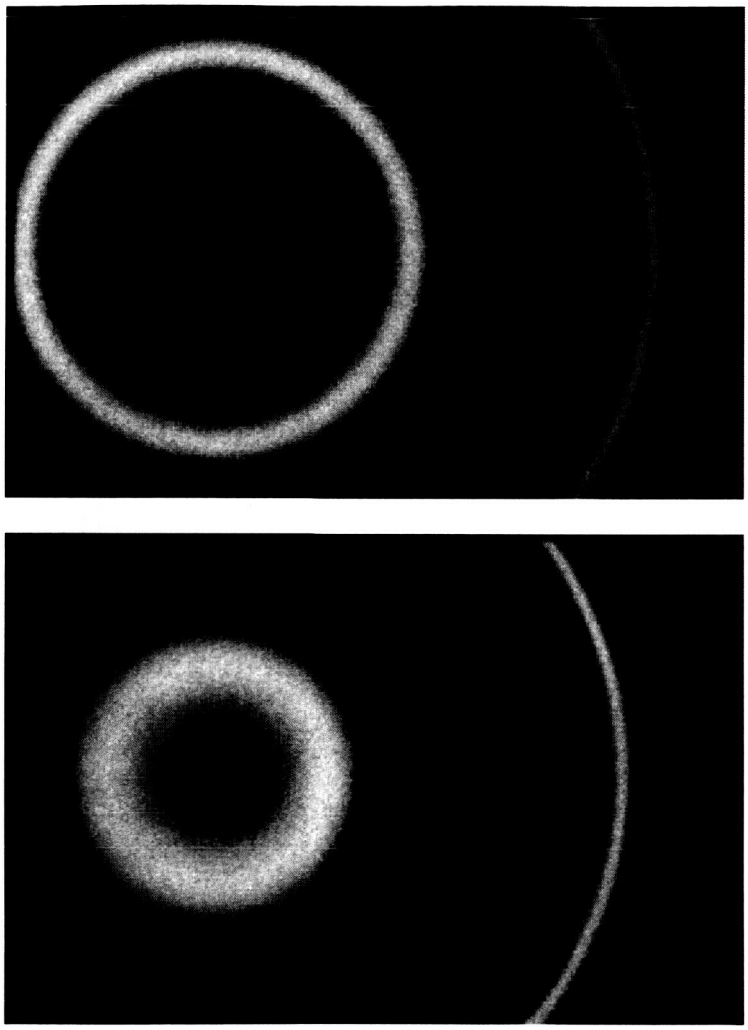

Fig. 4. Two images obtained from with different voltages applied to the piezo-electric stack. (Top) 0 V. (bottom) 150 V.

Fig. 5 displays a series of spectra reduced from the set of images represented by the above noted animation. The fringe corresponding to Fig 4 (top) has the largest initial bin number, or diameter. Two fringes are shown in both the images and in the spectra, though the outermost fringe is only partially recorded. An electronic bias level of 340 ADU was manually set in the CCD detector/controller by adjusting the appropriate potentiometer. A low order polynomial was fit to each of the two fringes in the sequence, supplying an estimate of the apex position of each peak relative to the fringe center. These results are displayed in Fig. 6. Both fringe sets appear to shift at a similar rate.

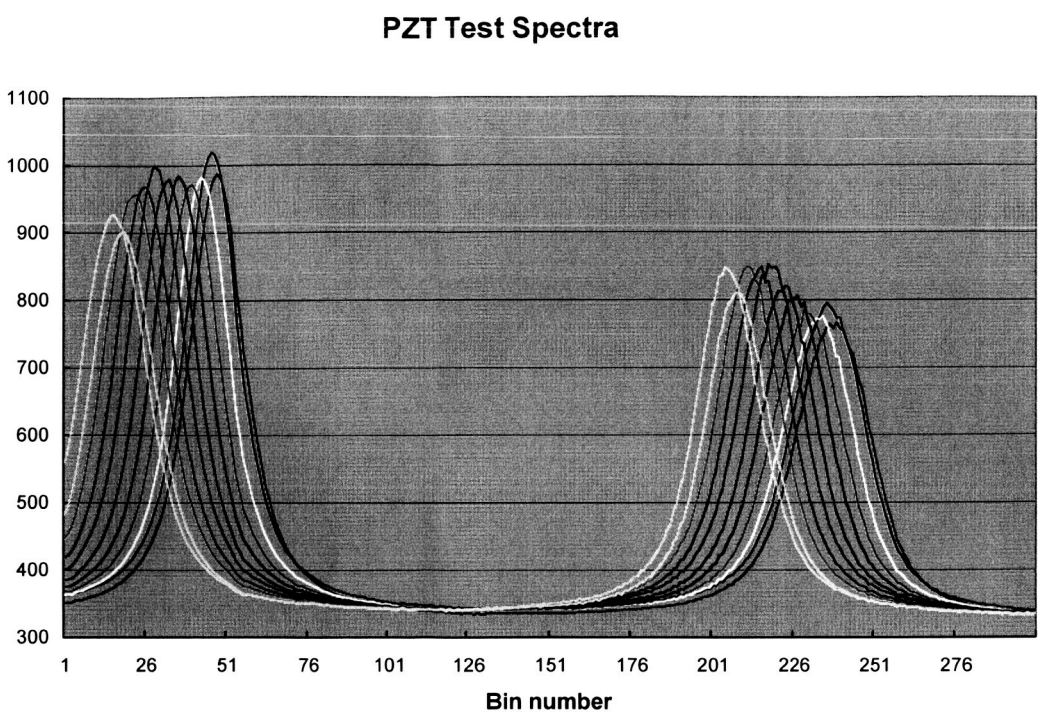

Fig. 5. Radially reduced spectra obtained from the animation series. The sequence begins with the rightmost fringe and covers the full range of control of the piezo-electric stack.

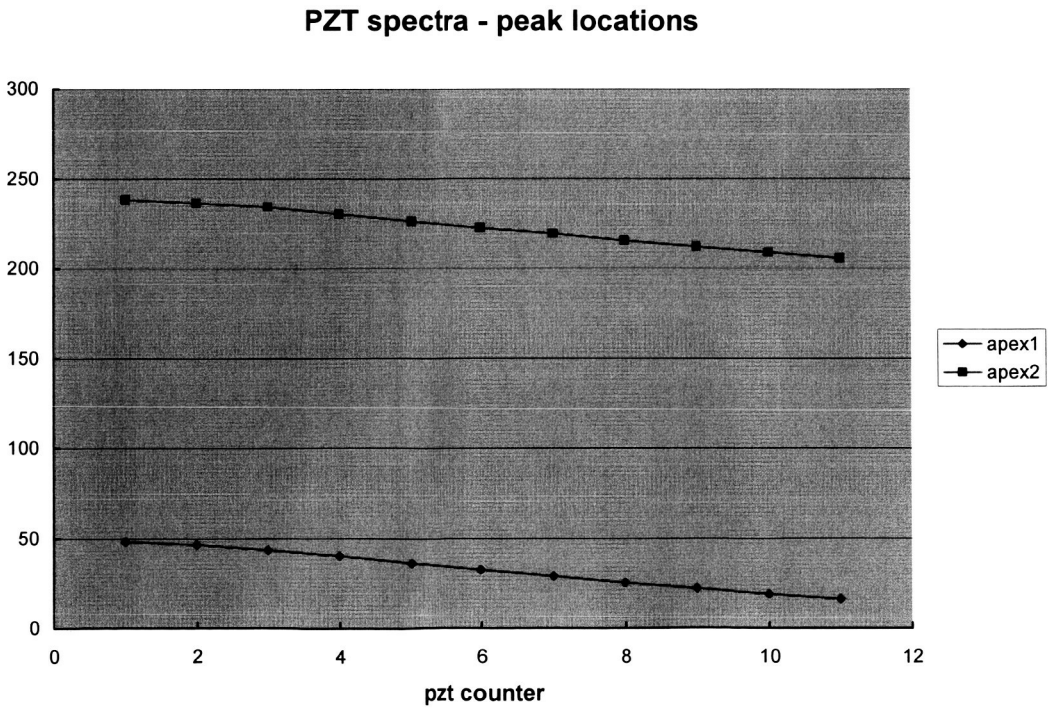

Fig. 6. Spectral peak locations determined for both fringes in the series of Fig. 5.

Closer examination of the rate of change of the apex positions of the fringe peaks is given by fitting the fringe peak trends with a low order polynomial, as shown in Fig. 7. There appears to be a small but subtle variation, suggested in the lower orders of the polynomial fit. By calculating the difference between the two fringe apices in each image, it is possible to characterize this difference as a function of applied voltage, as shown in Fig. 8. An apparent second order effect is evident suggesting that there is a non-linear variation across the etalon as greater force is exerted onto the top glass flat. The data points corresponding to Fig. 7 and 8 are shown in Table 1. The corresponding change in wavelength is tabulated in *delta d1 (Å)* and *delta d2 (Å)* indicating that a full 17.4 μm expansion of the piezo-electric stack shifts the fringe pattern by approximately 17% of a free spectral range or more than 500 Å. Fig. 9 displays this shift as a function of applied voltage.

file	Volts	apex1	apex2	delta apex	delta n1	delta n2	delta d1 (Å)	delta d2 (Å)
1	0	47.85	238.10	190.25				
2	15	46.25	236.19	189.94	-0.008	-0.010	26.58	31.75
3	30	43.23	234.04	190.81	-0.024	-0.021	76.90	67.61
4	45	39.85	230.13	190.28	-0.042	-0.042	133.11	132.60
5	60	36.13	226.03	189.90	-0.062	-0.063	195.03	200.89
6	75	32.48	222.56	190.09	-0.081	-0.082	255.89	258.61
7	90	28.84	219.18	190.34	-0.100	-0.100	316.47	314.97
8	105	25.35	215.39	190.04	-0.118	-0.119	374.62	378.08
9	120	22.04	211.79	189.75	-0.136	-0.138	429.66	437.89
10	135	18.70	208.63	189.93	-0.153	-0.155	485.32	490.59
11	150	15.97	205.46	189.49	-0.168	-0.172	530.73	543.28

Table 1. Reduced data from a sample PZT run. The individual image files are listed in column 1, while their associated stack voltages are in column 2. The fitted locations of the two fringe peaks and their difference are shown in the next columns. The fractional shift of the apex positions relative to the apex location at V = 0 are tabulated in the next two columns and translated into a wavelength shift in the final two columns on the right.

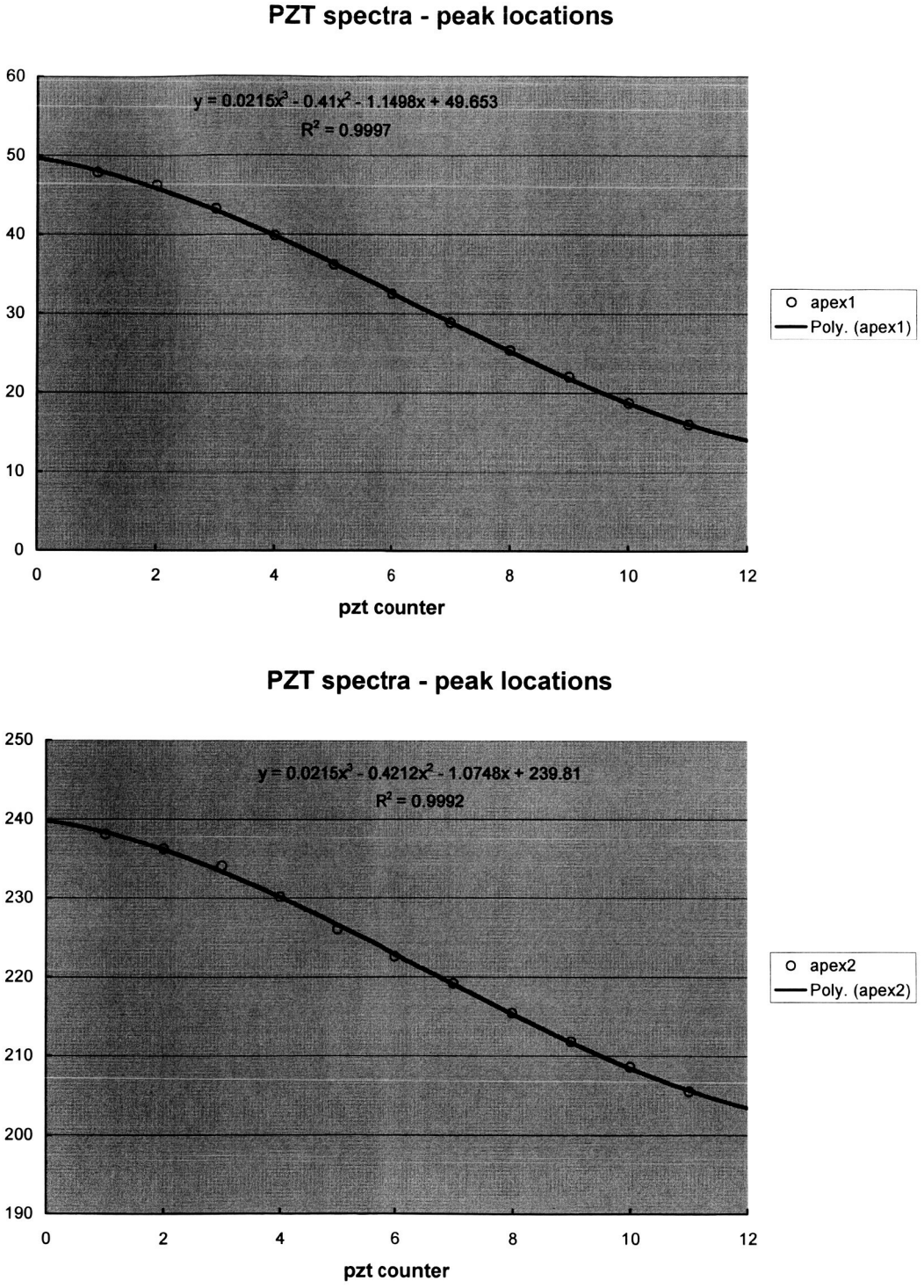

Fig. 7. Trend in spectral peak location as a function of PZT voltage: (top) innermost fringe. (bottom) outermost fringe. A low order polynomial fit describes the trend as a function of PZT file (or applied voltage).

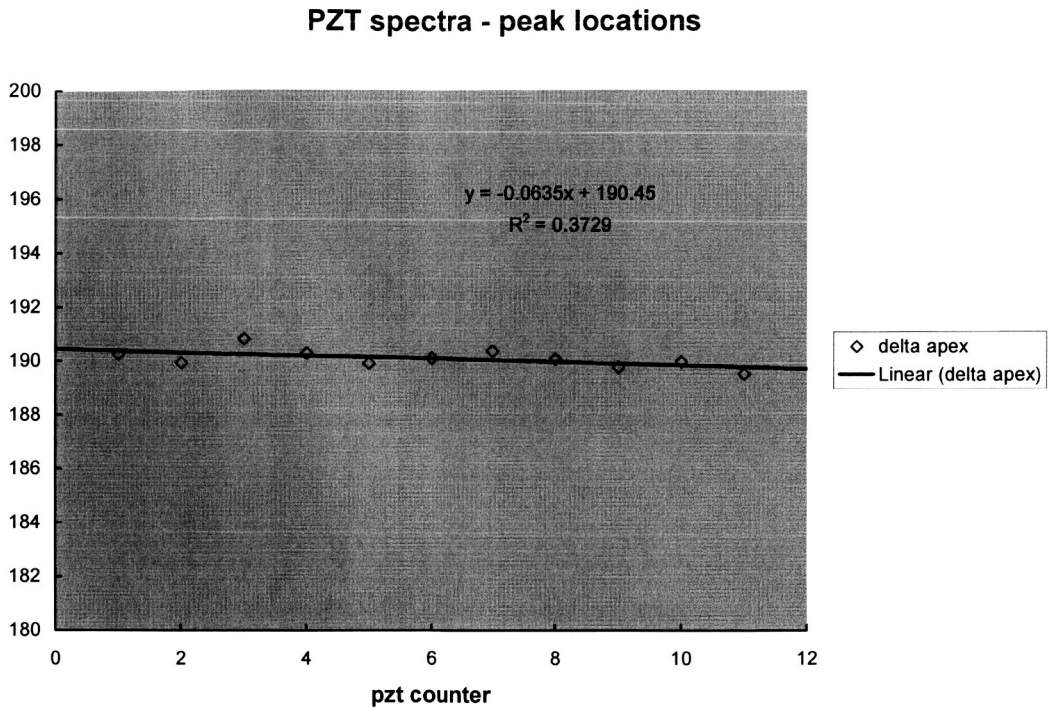

Fig. 8. Trend of the difference between adjacent fringe peak locations as a function of PZT image (applied voltage).

Fig. 9. Displacement of fringe peaks in terms of wavelength in Ångstroms.

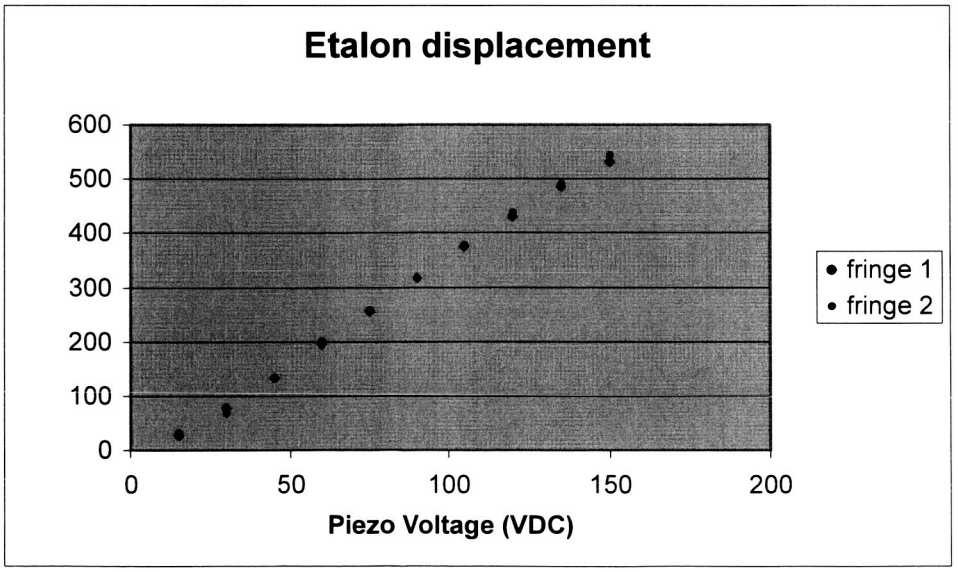

4. FINESSE

The effective finesse of the Fabry Perot etalon prior to the installation of the piezo-electric stack was compromised by the stresses imposed by the etalon mount. The effective finesse may be measured by determining the ratio between the distance between two adjacent fringe peaks and the full-width at the half-maximum level of a fringe. Fig. 10 displays the results of this calculation. At zero applied voltage, the effective finesse is near 10, similar to the results for the HRDI etalon as flown. As the applied voltage increases, the effective finesse deteriorates, indicating that the etalon is being further deformed.

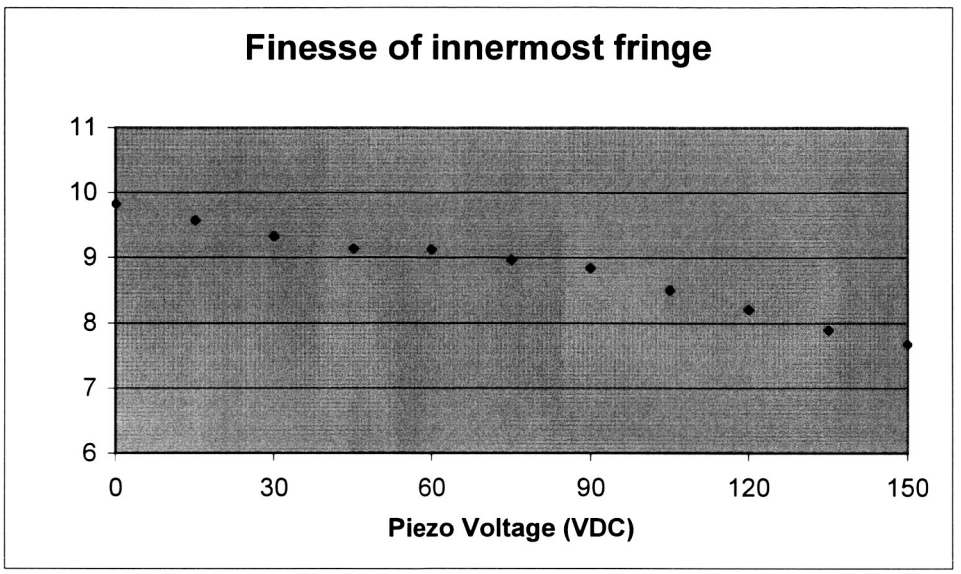

Fig. 10. The effective finesse of the innermost fringe as a function of applied voltage.

5. CONCLUSIONS

An experiment has been performed to measure the effective plate figure resulting from deformation due to the application of a force against the center of a Fabry Perot etalon. A piezo-electric stack was used to deform the outside of one glass flat, 13.2 cm in diameter, by up to 17.4 μm against a 6.5 x 6.5 mm^2 area resulting in a shift of 17% of a free spectral range in fringe location. The shift was accompanied with deterioration in the effective finesse of the etalon by about 20%. This study has clearly shown that a force applied to the center of an etalon can modify the plate figure.

References

1. G. Hernandez, *Fabry-Perot Interferometers* (Cambridge University Press, Cambridge, 1986).
2. W. R. Skinner, P. B. Hays, H. J. Grassl, D. A. Gell, M. D. Burrage, A. R. Marshall, and D. A. Ortland, "The high resolution Doppler imager on the upper atmosphere research satellite," SPIE **2266**, 281-293, 1994.
3. T. L. Killeen, W. R. Skinner, R. M. Johnson, C. J. Edmonson, Q. Wu, R. J. Niciejewski, H. J. Grassl, D. A. Gell, P. E. Hansen, J. D. Harvey, and J. F. Kafkalidis, "TIMED Doppler interferometer (TIDI)," SPIE **3756**, 289-301, 1999.
4. R. J. Niciejewski, T. L. Killeen, and M. Turnbull, "Ground-based Fabry-Pérot interferometry of the terrestrial nightglow with a bare charge-coupled device: remote field site deployment," Opt. Eng. **33**, 457-465, 1994.